

Formation of Metal Clusters or Nitrogen-Bridged Adducts by Reaction of a Bis(amino)stannylene with Halides of Two-Valent Transition Metals

Michael Veith,* Alice Müller, Lothar Stahl, Martin Nötzel, Maria Jarczyk, and Volker Huch

Institute for Inorganic Chemistry, University of the Saarland, D-66041 Saarbrücken, Germany

Received January 5, 1996[⊗]

When the cyclic bis(amino)stannylene $\text{Me}_2\text{Si}(\text{NtBu})_2\text{Sn}$ is allowed to react with metal halides MX_2 ($\text{M} = \text{Cr}, \text{Fe}, \text{Co}, \text{Zn}$; $\text{X} = \text{Cl}, \text{Br}$ [Zn]) adducts of the general formula $[\text{Me}_2\text{Si}(\text{NtBu})_2\text{Sn}\cdot\text{MX}_2]_n$ are obtained. The compounds are generally dimeric ($n = 2$) except the ZnBr_2 adduct, which is monomeric in benzene. The crystal structures of $[\text{Me}_2\text{Si}(\text{NtBu})_2\text{Sn}\cdot\text{CoCl}_2]_2$ (triclinic, space group $\bar{P}1$; $a = 8.620(9)$ Å, $b = 9.160(9)$ Å, $c = 12.280(9)$ Å, $\alpha = 101.2(1)^\circ$, $\beta = 97.6(1)^\circ$, $\gamma = 105.9(1)^\circ$, $Z = 1$) and of $[\text{Me}_2\text{Si}(\text{NtBu})_2\text{Sn}\cdot\text{ZnCl}_2]_2$ (monoclinic, space group $P2_1/c$; $a = 8.156(9)$ Å, $b = 16.835(12)$ Å, $c = 13.206(9)$ Å, $\beta = 94.27(6)^\circ$, $Z = 2$) were determined by X-ray diffraction techniques. The two compounds form similar polycyclic, centrosymmetrical assemblies of metal atoms bridged by chlorine or nitrogen atoms. While in the case of the cobalt compound Co is pentacoordinated by three chlorine and two nitrogen atoms, in the zinc derivative Zn is almost tetrahedrally coordinated by three chlorine atoms and one nitrogen atom. The iron derivative $[\text{Me}_2\text{Si}(\text{NtBu})_2\text{Sn}\cdot\text{FeCl}_2]_2$ seems to be isostructural with the cobalt compound as can be deduced from the crystal data (triclinic, $a = 8.622(7)$ Å, $b = 9.158(8)$ Å, $c = 12.353(8)$ Å, $\alpha = 101.8(1)^\circ$, $\beta = 96.9(1)^\circ$, $\gamma = 105.9(1)^\circ$, $Z = 1$). If NiBr_2 , PdCl_2 , or PtCl_2 is combined with the stannylene, the reaction product is totally different: 4 equiv of the stannylene are coordinating per metal halide, forming the molecular compound $[\text{Me}_2\text{Si}(\text{NtBu})_2\text{Sn}]_4\text{MX}_2$, which crystallizes with half a mole of benzene per molecular formula. The crystal structures of $[\text{Me}_2\text{Si}(\text{NtBu})_2\text{Sn}]_4\cdot\text{NiBr}_2\cdot\frac{1}{2}\text{C}_6\text{H}_6$ (tetragonal, space group $I4_1/a$, $a = b = 43.86(4)$ Å, $c = 14.32(2)$ Å, $Z = 16$) and $[\text{Me}_2\text{Si}(\text{NtBu})_2\text{Sn}]_4\cdot\text{PdCl}_2\cdot\frac{1}{2}\text{C}_6\text{H}_6$ (tetragonal, space group $I4_1/a$, $a = b = 43.99(4)$ Å, $c = 14.318(14)$ Å, $Z = 16$) reveal the two compounds to be isostructural. The molecules have an inner Sn_4M pentametallic core (mean distances: $\text{Sn}-\text{Ni}$ 2.463 Å, $\text{Sn}-\text{Pd}$ 2.544 Å) with the transition metal in the center of a slightly distorted square formed by the four tin atoms, the distortion from planarity resulting in a weak paramagnetism of $0.2 \mu_{\text{B}}$ for the nickel compound. The halogen atoms form bridges between two of the tin atoms and have no bonding interaction with the transition metal. The nickel compound has also been prepared by direct interaction of Br_2 or NR_4Br_3 with $[\text{Me}_2\text{Si}(\text{NtBu})_2\text{Sn}]_4\text{Ni}$ as a minor product, the main products being $\text{Me}_2\text{Si}(\text{NtBu})_2\text{Sn}(\text{NtBu})_2\text{SiMe}_2$, $\text{Me}_2\text{Si}(\text{NtBu})_2\text{SnBr}_2$, NiBr_2 and SnBr_2 . Other metal clusters have been obtained by the reaction of $\text{Me}_2\text{Si}(\text{NtBu})_2\text{Sn}$ with tetrakis(triphenylphosphine)palladium or by the reaction of $\text{Me}_2\text{Si}(\text{NtBu})_2\text{Ge}$ with $\text{RhCl}(\text{PPh}_3)_3$. In the first case $\text{Ph}_3\text{PPd}[\text{Sn}(\text{NtBu})_2\text{SiMe}_2]_3\text{PdPPh}_3$ (rhombohedral, space group $R3c$, $a = b = 21.397(12)$ Å, $c = 57.01(5)$ Å, $\alpha = \beta = 90^\circ$, $\gamma = 120^\circ$, $Z = 12$) is formed and is characterized by X-ray techniques to be composed of a central PdSn_3Pd trigonal bipyramid with the tin atoms occupying the equatorial positions ($\text{Pd}-\text{Sn} = 2.702(5)$ Å). In the second reaction all the triphenylphosphine ligands are replaced from rhodium and $\text{Rh}[\text{Ge}(\text{NtBu})_2\text{SiMe}_2]_4\text{Cl}$ is formed (monoclinic, space group $P2_1/n$, $a = 12.164(2)$ Å, $b = 23.625(5)$ Å, $c = 24.128(5)$ Å, $\beta = 102.74(3)^\circ$, $Z = 4$). The central core of this molecule is made up of a rhodium atom which is almost square planarly coordinated by the germanium atoms, two of which are bridged by chlorine (mean $\text{Ge}-\text{Rh} = 2.355$ Å).

Introduction

The bis(amino)stannylene $\text{Me}_2\text{Si}(\text{NtBu})_2\text{Sn}$ (**1**) can behave as an efficient donor to transition metals, which was demonstrated by the synthesis and characterization of the complexes $\text{Rh}[\text{Sn}(\text{NtBu})_2\text{SiMe}_2]_3\text{Cl}^1$ or $\text{Ni}[\text{Sn}(\text{NtBu})_2\text{SiMe}_2]_4$.² In both compounds, the central transition metal is coordinated by five or four tin atoms, the tin(II) atom acting as an electron donor *via* its lone pair. On the other hand, we have noticed that the whole atom arrangement N_2Sn in **1** may act as a tridentate ligand toward metal halides, $\text{Me}_2\text{Si}(\text{NtBu})_2\text{Sn}\cdot(\text{SnCl})^+\text{SnCl}_3^-$ being a good example.³ In this case the two nitrogen atoms of the ring compound **1** act as donors toward the tin atom of the SnCl^+ unit while the tin atom of **1** is coordinated to the chlorine of SnCl^+ (displaying electron acceptor properties).

From these findings it seemed worthwhile to have a closer look at the ligating properties of the bis(amino)stannylene **1** *vs* simple transition metal halides of the type MX_2 . These metal halides could act either as simple acceptors *via* their metal atoms or as a combined acid–base system. Using the simple Pearson's hard and soft acid rule,⁴ we should get $\text{N} \rightarrow \text{M}$ interactions with small cations and $\text{Sn} \rightarrow \text{M}$ interactions with bigger and heavier transition metals. In order to test these predictions, we chose the following series: CrCl_2 , FeCl_2 , CoCl_2 , NiCl_2 , ZnCl_2 , NiBr_2 , ZnBr_2 as well as PdCl_2 and PtCl_2 in the nickel group. During these investigations we also had a look at the reaction of $\text{Ni}[\text{Sn}(\text{NtBu})_2\text{SiMe}_2]_4$ with Br_2 , as will become evident from the results obtained at this stage. To conclude our survey we have also included the reaction of **1** with $\text{Pd}[\text{PPh}_3]_4$ and of $\text{Me}_2\text{Si}(\text{NtBu})_2\text{Ge}$ with $[\text{Rh}(\text{PPh}_3)_3]\text{Cl}$ as the clusters formed in these reactions could have differences from or similarities with the cluster compounds obtained from the simple reactions of **1** with MX_2 .

[⊗] Abstract published in *Advance ACS Abstracts*, May 15, 1996.

- (1) Veith, M.; Stahl, L.; Huch, V. *Inorg. Chem.* **1989**, *28*, 3278.
- (2) Veith, M.; Stahl, L.; Huch, V. *J. Chem. Soc., Chem. Commun.* **1990**, 359.
- (3) Veith, M.; Huch, V.; Lisowsky, R.; Hobein, P. *Z. Anorg. Allg. Chem.* **1989**, *569*, 43.

(4) Pearson, R. G. *Coord. Chem. Rev.* **1990**, *100*, 403.

Table 1. Crystallographic Data for 4, 5, 7, 8, 10, 11

	4	5	7	8	10	11
formula	C ₂₀ H ₄₈ Cl ₄ Co ₂ N ₄ Si ₂ Sn ₂	C ₂₀ H ₄₈ Cl ₄ N ₄ Si ₂ Sn ₂ Zn ₂	C ₄₀ H ₉₆ Br ₂ N ₈ NiSi ₄ Sn ₄ · 0.5C ₆ H ₆	C ₄₀ H ₉₆ Cl ₂ N ₈ PdSi ₄ Sn ₄ · 0.5C ₆ H ₆	C ₄₀ H ₉₆ ClGe ₄ N ₈ RhSi ₄ · C ₇ H ₈	C ₆₆ H ₁₀₂ N ₆ P ₂ Pd ₂ Si ₃ Sn ₃
fw.	897.86	910.75	1533.95	1492.83	1322.46	1694.62
a, Å	8.620(9)	8.156(9)	43.86(4)	43.99(4)	12.164(2)	21.397(12)
b, Å	9.160(9)	16.835(12)	43.86(4)	43.99(4)	23.625(5)	21.397(12)
c, Å	12.280(9)	13.206(9)	14.32(2)	14.318(14)	24.128(5)	57.01(5)
α, deg	101.2(1)	90	90	90	90	90
β, deg	97.6(1)	94.27(6)	90	90	102.74(3)	90
γ, deg	105.9(1)	90	90	90	90	120
V, Å ³	897(2)	1808(3)	27553(50)	27707(45)	6763(2)	22605(26)
Z	1	2	16	16	4	12
space group	P $\bar{1}$	P2 ₁ /c	I4 ₁ /a	I4 ₁ /a	P2 ₁ /c	R3c
d _{calc.} , g/cm ⁻³	1.663	1.673	1.441	1.394	1.299	1.494
μ(Mo Kα) ^b , mm ⁻¹	2.67	3.05	2.96	1.85	2.140	1.579
no. of reflns	1673	3164	5857	9209	8844	3985
no. of params	155	155	344	456	538	494
I _{obs} > nσ	2	2	2	2	2	2
largest diff. peak and hole, e Å ⁻³	0.904; -1.265	0.657; -0.438	0.757; -0.574	0.877; -0.493	0.689; -0.323	0.740; -0.935
R ₁	0.037	0.043	0.090	0.045	0.033	0.038
wR ₂ ^a	0.099	0.105	0.157	0.127	0.083	0.093

$$^a wR_2 = (\sum w(F_o^2 - F_c^2)^2 / \sum w(F_o^2)^2)^{1/2}; w = 1/[\sigma^2(F_o^2) + (aP)^2 + bP + d + e \sin \theta]; P = (F_o + 2F_c^2)/3. ^b \lambda = 0.71073 \text{ \AA}.$$

Experimental Section

All manipulations were done on a modified Schlenk-type vacuum line, under an atmosphere of prepurified nitrogen gas. The NMR (¹H, ¹³C, ³¹P, ¹¹⁹Sn, ¹⁹⁵Pt) spectra were recorded on Bruker AC 200 and AM 400 instruments, using benzene-*d*₆ as the lock solvent. Proton and carbon NMR spectra are referenced relative to TMS, and the ¹¹⁹Sn and ¹⁹⁵Pt spectra, to tetramethyltin and potassium hexachloroplatinate, respectively. The phosphorus signals are given relative to P(OMe)₃ at 0.00 ppm. Mass spectra were measured with a Finnigan MAT 90 instrument, operating in either the EI (70 eV) or CI (methane) mode. Elemental analyses (C, H, N) were performed by Beller, Göttingen, Germany. Melting points (uncorrected) were determined by sealing single crystals of the compounds under an inert atmosphere inside melting point capillaries. The data sets for the single-crystal X-ray studies were collected on a fully automated Siemens/Stoe AED2 four-circle diffractometer. All calculations were performed on a Digital Corporation VAX system, with the help of SHELXS 86, SHELXL 93 and SHELXTL-PLUS programs. The specific data of the crystals and the refinements are collected in Table 1, some results of the structure determinations are assembled in Table 2–5.

The graphical representations of the molecular structures were drawn by using either the SCHAKAL program or the XP routine of the SHELXTL-PLUS package. The Ge(II) and Sn(II) compounds Me₂-Si(NtBu)₂Ge and Me₂Si(NtBu)₂Sn were prepared according to literature methods.^{5,6}

General procedure for the reaction of transition metal halides with the cyclic bis(amino)stannylenes **1**. To a suspension of 2.0 mmol of anhydrous MX₂ (CrCl₂, FeCl₂, CoCl₂, NiCl₂, NiBr₂, ZnCl₂, ZnBr₂, PdCl₂, PtCl₂), in 15 mL of toluene (benzene), was added a solution of 2.0 mL (8.0 mmol) of Me₂Si(NtBu)₂Sn in 10 mL of toluene (benzene). In each case the reaction mixture changed its color with exception of NiCl₂ which gave no reaction, the components being recovered unchanged even after refluxing for 10 days (NMR evidence). Most of the metal halides dissolved within 30 min, and only NiBr₂ and PtCl₂ were heated for 48 h at 40 °C and 30 min at 60 °C, respectively. Upon removal of the solvent and excess of **1** in vacuo a colored solid remained. This was taken up in a minimum amount of hexane and cooled to -20 °C. The products crystallized from these solutions and could be easily separated.

Cr₂[Sn(NtBu)₂SiMe₂]₂Cl₄ (2): pale green, rod-shaped crystals; yield 0.63 g (72%); mp 140 °C dec; molecular weight (cryoscopic in benzene) 843 g/mol; paramagnetic compound, 2.48 μ_B (Evans method).

(5) Veith, M. *Angew. Chem.* **1975**, *87*, 287.; *Angew. Chem., Int. Ed. Engl.* **1975**, *14*, 263.

(6) Veith, M.; Grosser, M. *Z. Naturforsch.* **1982**, *37B*, 1375.

Table 2. Selected Bond Lengths (Å) and Bond Angles (deg) for 4 and 5

Compound 4			
Sn–N(1)	2.165(6)	Co–Cl(2)#1	2.337(5)
Sn–Cl(1)	2.606(4)	Sn–N(2)	2.195(5)
Co–N(2)	2.156(6)	Co–N(1)	2.342(5)
Co–Cl(1)	2.365(3)	Si–N(1)	1.752(6)
Co–Cl(2)	2.379(3)	Si–N(2)	1.765(5)
mean:			
C–N	1.487(9)	C–C	1.53(1)
N(1)–Sn–N(2)	67.3(2)	Sn–N(1)–Co	81.7(2)
N(1)–Sn–Cl(1)	89.3(2)	C(1)–N(2)–Si	128.2(4)
N(2)–Sn–Cl(1)	87.6(2)	C(1)–N(2)–Co	127.6(4)
N(2)–Co–Cl(2)#1	149.8(2)	Si–N(2)–Co	87.9(2)
N(2)–Co–N(1)	64.8(2)	C(1)–N(2)–Sn	122.4(4)
Cl(2)#1–Co–N(1)	97.3(2)	Si–N(2)–Sn	92.8(2)
N(2)–Co–Cl(1)	95.1(2)	Co–N(2)–Sn	85.4(2)
Cl(2)#1–Co–Cl(1)	110.24(14)	Si–N(1)–Sn	94.2(2)
C(2)–N(1)–Si	130.0(4)	C(2)–N(1)–Co	131.0(4)
C(2)–N(1)–Sn	122.5(4)	Si–N(1)–Co	82.5(2)
N(1)–Co–Cl(1)	91.3(2)	N(1)–Co–Cl(2)	160.6(2)
N(2)–Co–Cl(2)	103.9(2)	Cl(1)–Co–Cl(2)	105.75(13)
Cl(2)#1–Co–Cl(2)	85.40(13)	Co–Cl(1)–Sn	72.68(10)
N(1)–Si–N(2)	86.8(3)	Co#1–Cl(2)–Co	94.60(13)
Compound 5			
Si–N(2)	1.729(7)	Sn–Cl(2)	2.791(3)
Si–N(1)	1.799(6)	Zn–N(1)	2.014(6)
N(1)–C(1)	1.514(9)	Zn–Cl(2)	2.309(3)
N(2)–C(2)	1.483(11)	Zn–Cl(1)	2.309(3)
Sn–N(2)	2.033(7)	Zn–Cl(1)#1	2.367(3)
Sn–N(1)	2.252(6)		
N(2)–Sn–N(1)	74.0(2)	Zn–Cl(2)–Sn	78.19(8)
N(2)–Sn–Cl(2)	94.7(2)	C(1)–N(1)–Si	123.9(5)
N(1)–Sn–Cl(2)	80.4(2)	C(1)–N(1)–Zn	112.4(4)
N(1)–Zn–Cl(2)	98.5(2)	Si–N(1)–Zn	111.3(3)
N(1)–Zn–Cl(1)	123.5(2)	C(1)–N(1)–Sn	115.1(4)
Cl(2)–Zn–Cl(1)	116.72(10)	Si–N(1)–Sn	90.9(3)
N(1)–Zn–Cl(1)#1	126.4(2)	Zn–N(1)–Sn	98.6(2)
Cl(2)–Zn–Cl(1)#1	102.44(11)	C(2)–N(2)–Si	131.6(6)
Cl(1)–Zn–Cl(1)#1	88.90(10)	C(2)–N(2)–Sn	126.8(6)
N(2)–Si–N(1)	94.2(3)	Si–N(2)–Sn	100.8(3)
Zn–Cl(1)–Zn#1	91.10(10)		

UV-spectrum: λ (max) = 709 nm (ε = 321). Anal. Calcd for C₂₀H₄₈-Cl₄Cr₂N₄Si₂Sn₂, 883.98 g/mol: C, 27.18; H, 5.47; N, 6.34; Sn, 26.85. Found: C, 27.16, H, 5.51; N, 6.33; Sn, 24.57.

Fe₂[Sn(NtBu)₂SiMe₂]₂Cl₄ (3): brown-yellow, rod-shaped crystals; yield 0.70 g (79%); mp 125 °C dec; molecular weight (cryoscopic)

Table 3. Selected Bond Lengths (Å) and Bond Angles (deg) of **7** and **8**

Compound 7			
Sn(1)–N(1)	1.99(2)	Sn(3)–N(6)	2.03(2)
Sn(4)–Br(2)	2.789(4)	Sn(4)–N(7)	2.02(2)
Sn(3)–Ni	2.467(4)	Sn(3)–Br(2)	2.813(4)
Si(1)–N(1)	1.72(2)	Si(3)–N(5)	1.70(2)
Si(1)–N(2)	1.75(2)	Si(3)–N(6)	1.74(2)
Si(2)–N(3)	1.70(2)	Sn(2)–Ni	2.466(4)
Si(2)–N(4)	1.75(2)	Sn(2)–N(4)	2.03(2)
Sn(1)–N(2)	2.03(2)	Sn(2)–N(3)	2.03(3)
Sn(1)–Ni	2.460(4)	Sn(2)–Br(1)	2.847(4)
Sn(1)–Br(1)	2.776(4)	Sn(3)–N(5)	2.00(2)
Sn(4)–Ni	2.459(4)		
Sn(4)–N(8)	2.02(2)		
N(1)–Sn(1)–N(2)	76.5(9)	N(6)–Sn(3)–Br(2)	99.2(6)
N(1)–Sn(1)–Ni	129.6(7)	Ni–Sn(3)–Br(2)	97.16(14)
N(2)–Sn(1)–Ni	143.2(7)	N(7)–Sn(4)–N(8)	74.0(9)
N(1)–Sn(1)–Br(1)	98.5(7)	N(7)–Sn(4)–Ni	145.6(7)
N(2)–Sn(1)–Br(1)	101.3(7)	N(8)–Sn(4)–Ni	130.9(6)
Ni–Sn(1)–Br(1)	99.51(14)	N(7)–Sn(4)–Br(2)	99.0(6)
N(4)–Sn(2)–N(3)	76.8(9)	N(8)–Sn(4)–Br(2)	101.2(6)
N(4)–Sn(2)–Ni	127.5(7)	Ni–Sn(4)–Br(2)	97.98(14)
N(3)–Sn(2)–Ni	149.2(7)	Sn(4)–Ni–Sn(1)	162.9(2)
N(4)–Sn(2)–Br(1)	96.9(6)	Sn(4)–Ni–Sn(2)	93.9(2)
N(3)–Sn(2)–Br(1)	97.7(7)	Sn(1)–Ni–Sn(2)	87.7(2)
Ni–Sn(2)–Br(1)	97.48(14)	Sn(4)–Ni–Sn(3)	88.8(2)
N(5)–Sn(3)–N(6)	75.6(8)	Sn(1)–Ni–Sn(3)	94.3(2)
N(5)–Sn(3)–Ni	142.0(6)	Sn(2)–Ni–Sn(3)	163.7(2)
N(6)–Sn(3)–Ni	134.4(6)	Sn(1)–Br(1)–Sn(2)	74.72(12)
N(5)–Sn(3)–Br(2)	99.8(6)	Sn(4)–Br(2)–Sn(3)	75.98(12)
Compound 8			
Pd–Sn(1)	2.542(2)	Sn(4)–Cl(1)	2.652(3)
Pd–Sn(3)	2.542(2)	Sn(4)–N(7)	2.018(8)
Pd–Sn(4)	2.544(2)	Sn(4)–N(8)	2.025(8)
Pd–Sn(2)	2.547(2)	Si(1)–N(1)	1.733(9)
Sn(1)–N(1)	2.043(8)	Si(1)–N(2)	1.753(10)
Sn(1)–N(2)	2.045(8)	Si(2)–N(3)	1.733(9)
Sn(1)–Cl(2)	2.617(3)	Si(2)–N(4)	1.740(9)
Sn(2)–N(4)	2.027(8)	Si(3)–N(5)	1.727(11)
Sn(2)–N(3)	2.028(8)	Si(3)–N(6)	1.731(10)
Sn(2)–Cl(1)	2.661(3)	Si(4)–N(7)	1.732(9)
Sn(3)–N(5)	2.023(9)	Si(4)–N(8)	1.734(9)
Sn(3)–N(6)	2.033(9)		
Sn(3)–Cl(2)	2.699(3)		
N(3)–Sn(2)–Cl(1)	102.6(3)	Sn(1)–Pd–Sn(3)	85.52(8)
Pd–Sn(2)–Cl(1)	95.63(9)	Sn(1)–Pd–Sn(4)	164.45(4)
N(5)–Sn(3)–N(6)	76.5(4)	Sn(3)–Pd–Sn(4)	96.31(8)
N(5)–Sn(3)–Pd	149.4(3)	Sn(1)–Pd–Sn(2)	95.76(7)
N(6)–Sn(3)–Pd	126.5(3)	Sn(3)–Pd–Sn(2)	165.30(4)
N(5)–Sn(3)–Cl(2)	100.9(3)	Sn(4)–Pd–Sn(2)	86.38(7)
N(6)–Sn(3)–Cl(2)	98.4(3)	N(1)–Sn(1)–N(2)	77.0(4)
Pd–Sn(3)–Cl(2)	95.48(9)	N(1)–Sn(1)–Pd	128.0(3)
N(7)–Sn(4)–N(8)	76.3(3)	N(2)–Sn(1)–Pd	143.5(3)
N(7)–Sn(4)–Pd	145.2(2)	N(1)–Sn(1)–Cl(2)	100.8(3)
N(8)–Sn(4)–Pd	129.0(2)	N(2)–Sn(1)–Cl(2)	103.4(3)
N(7)–Sn(4)–Cl(1)	101.6(2)	Pd–Sn(1)–Cl(2)	97.54(9)
N(8)–Sn(4)–Cl(1)	102.1(2)	N(4)–Sn(4)–N(3)	76.5(3)
Pd–Sn(4)–Cl(1)	95.91(9)	N(4)–Sn(2)–Pd	132.6(2)
Sn(4)–Cl(1)–Sn(2)	81.96(10)	N(3)–Sn(2)–Pd	141.9(2)
Sn(1)–Cl(2)–Sn(3)	80.97(10)	N(4)–Sn(2)–Cl(1)	100.9(3)

874 g/mol; paramagnetic compound, 5.46 μ_B . Crystal data (single-crystal X-ray diffraction): triclinic, $a = 8.622(7)$, $b = 9.158(8)$, $c = 12.353(8)$ Å; $\alpha = 101.8(1)$, $\beta = 96.9(1)$, $\gamma = 105.9(1)^\circ$. Anal. Calcd for $C_{20}H_{48}Cl_4Fe_2N_4Si_2Sn_2$, 891.68 g/mol: C, 26.94; H, 5.43; N, 6.28; Sn, 26.62. Found: C, 27.03; H, 5.50; N, 6.33; Sn, 25.81.

Co₂[Sn(NtBu)₂SiMe₂]₂Cl₄ (4**):** dark blue, rod-shaped crystals; yield 0.83 g (92%); mp 80 °C dec; molecular weight (cryoscopic) 861 g/mol. MM (spectrum): peak of highest intensity and mass: 881(C₁₉H₄₅-³⁵Cl₃³⁷ClCoN₄Si₂¹¹⁸Sn₂, M – 15). Paramagnetic compound: 5.0 μ_B . UV-spectrum: $\lambda(\text{max}) = 707$ nm ($\epsilon = 289$). Anal. Calcd for $C_{20}H_{48}Cl_4Co_2N_4Si_2Sn_2$, 897.86 g/mol: C, 26.75; H, 5.39; N, 6.24; Co, 13.13. Found: C, 27.89; H, 5.57; N, 6.19; Co, 12.96.

Table 4. Selected Bond Lengths (Å) and Bond Angles (deg) of **10**

Rh–Ge(2)	2.3366(9)	Si(1)–C(11)	1.855(6)
Rh–Ge(1)	2.3368(7)	Si(2)–N(22)	1.727(4)
Rh–Ge(4)	2.3711(7)	Si(2)–N(21)	1.736(4)
Rh–Ge(3)	2.3756(8)	Si(2)–C(22)	1.851(6)
Ge(1)–N(12)	1.834(4)	Si(2)–C(21)	1.866(7)
Ge(1)–N(11)	1.839(4)	Si(3)–N(32)	1.723(4)
Ge(2)–N(21)	1.835(4)	Si(3)–N(31)	1.730(4)
Ge(2)–N(22)	1.835(4)	Si(3)–C(31)	1.868(6)
Ge(3)–N(32)	1.850(4)	Si(3)–C(32)	1.872(6)
Ge(3)–N(31)	1.854(4)	Si(4)–N(42)	1.720(5)
Ge(3)–Cl	2.5944(14)	Si(4)–N(41)	1.726(4)
Ge(4)–N(42)	1.850(4)	Si(4)–C(41)	1.868(6)
Ge(4)–N(41)	1.851(4)	Si(4)–C(42)	1.876(6)
Ge(4)–Cl	2.604(2)		
Si(1)–N(12)	1.727(4)		
Si(1)–N(11)	1.737(4)		
Ge(2)–Rh–Ge(4)	92.10(3)	Ge(3)–Cl–Ge(4)	77.34(4)
Ge(1)–Rh–Ge(4)	163.36(2)	N(12)–Si(1)–N(11)	88.2(2)
Ge(2)–Rh–Ge(3)	161.34(2)	N(12)–Si(1)–C(12)	114.8(3)
Ge(1)–Rh–Ge(3)	93.93(3)	N(11)–Si(1)–C(12)	115.1(3)
Ge(4)–Rh–Ge(3)	86.37(3)	N(12)–Si(1)–C(11)	113.9(3)
N(12)–Ge(1)–N(11)	82.1(2)	N(11)–Si(1)–C(11)	114.6(3)
N(12)–Ge(1)–Rh	130.57(13)	C(12)–Si(1)–C(11)	109.1(3)
N(11)–Ge(1)–Rh	147.37(13)	N(22)–Si(2)–N(21)	88.2(2)
N(21)–Ge(2)–N(22)	82.1(2)	N(22)–Si(2)–C(22)	115.2(3)
N(21)–Ge(2)–Rh	147.86(13)	N(32)–Si(3)–C(22)	114.5(3)
N(22)–Ge(2)–Rh	129.86(13)	N(21)–Si(2)–C(21)	114.5(3)
N(32)–Ge(3)–N(31)	81.4(2)	C(22)–Si(2)–C(21)	109.2(4)
N(32)–Ge(3)–Rh	137.24(13)	N(32)–Si(3)–N(31)	88.7(2)
N(31)–Ge(3)–Rh	132.95(12)	N(32)–Si(3)–C(31)	116.0(3)
N(32)–Ge(3)–Cl	102.34(14)	N(31)–Si(3)–C(31)	115.2(3)
N(31)–Ge(3)–Cl	96.47(12)	N(32)–Si(3)–C(32)	114.4(3)
Rh–Ge(3)–Cl	98.23(4)	N(31)–Si(3)–C(32)	115.2(3)
N(42)–Ge(4)–N(41)	81.4(2)	C(31)–Si(3)–C(32)	106.9(3)
N(42)–Ge(4)–Rh	134.02(14)	N(42)–Si(4)–N(41)	88.9(2)
N(41)–Ge(4)–Rh	136.09(13)	N(42)–Si(4)–C(41)	115.4(3)
N(42)–Ge(4)–Cl	96.39(13)	N(41)–Si(4)–C(41)	113.6(3)
N(41)–Ge(4)–Cl	102.86(13)	N(42)–Si(4)–C(42)	115.4(3)
Rh–Ge(4)–Cl	98.07(4)	N(41)–Si(4)–C(42)	116.0(3)

Zn₂[Sn(NtBu)₂SiMe₂]₂Cl₄ (5**):** pale yellow, prismatic crystals; yield 0.76 g (83%); mp 130 °C dec; molecular weight (cryoscopic) 892 g/mol. ¹H-NMR (benzene): 0.20 (s, 1.0, Si–CH₃), 0.62 (s, 1.0, Si–CH₃), 1.20 (s, 6.0, C–CH₃) ppm. MM (spectrum): peak of highest intensity and mass: 873 (C₂₀H₄₈N₄³⁵Cl₃¹¹⁸Sn₂⁶⁴Zn⁶⁸Zn, M – Cl). Anal. Calcd for $C_{20}H_{48}Cl_4N_4Si_2Sn_2Zn_2$, 910.75 g/mol: C, 26.38; H, 5.31; N, 6.15; Sn, 26.06. Found: C, 26.39; H, 5.31; N, 6.20; Sn, 26.30.

Zn[Sn(NtBu)₂SiMe₂]₂Br₂ (6**):** pale yellow, rod-shaped crystals; yield 0.88 g (81%); mp 125 °C dec; molecular weight (cryoscopic) 558 g/mol. ¹H-NMR (benzene): –0.04 (s, 1.0, Si–CH₃), 0.52 (s, 1.0, Si–CH₃), 1.09 (s, 6.0, C–CH₃) ppm. Anal. Calcd for $C_{10}H_{24}Br_2N_2Si_2SnZn$, 544.28 g/mol: C, 22.06; H, 4.44; N, 5.15; Sn, 21.81. Found: C, 22.16; H, 4.50; N, 5.12; Sn, 20.70.

Ni[Sn(NtBu)₂SiMe₂]₂Br₂ (7**):** dark red, rod-shaped crystals; yield 2.34 g (78%); mp 150 °C dec; molecular weight (cryoscopic) 1420 g/mol. ¹H-NMR (benzene): 0.42 (s, 1.0, Si–CH₃), 1.45 (s, 3.0, C–CH₃) ppm. ¹³C-NMR (benzene): 7.23 (s, 1.0, Si–CH₃); 36.72 (³J_{Sn–C} = 26.7 Hz, 15%, C–CH₃); 53.34 (s, 1.0, C–CH₃) ppm. ²⁹Si-NMR: 8.77 ppm. Small paramagnetism: 0.2 μ_B . UV-spectrum: $\lambda(\text{max}) = 380$ nm (sh, $\epsilon = 4147$), 333 nm ($\epsilon = 8955$). Anal. Calcd for $C_{43}H_{99}Br_2N_8NiSi_4Sn_4$ ($7 \cdot 0.5$ C₆H₆), 1533.95 g/mol: C, 33.67; H, 6.51; N, 7.30; Sn, 30.96; Ni, 3.83. Found: C, 32.53; H, 7.13; N, 7.12; Sn, 29.98; Ni, 3.18.

Pd[Sn(NtBu)₂SiMe₂]₂Cl₂ (8**):** dark red, rod-shaped crystals; yield 2.09 g (72%); mp 290 °C dec; molecular weight (cryoscopic) 1452 g/mol. ¹H-NMR (benzene): 0.44 (s, 1.0, Si–CH₃), 1.41 (s, 3.0, C–CH₃) ppm. ¹³C-NMR (benzene): 6.99 (s, 1.0, Si–CH₃), 7.83 (s, 1.0, Si–CH₃), 36.64 (s, 6.0, C–CH₃), 53.03 (s, 2.0, C–CH₃) ppm. ¹¹⁹Sn-NMR (benzene): 55.85 (s) ppm. Anal. Calcd for $C_{43}H_{99}Cl_2N_8PdSi_4Sn_4$ ($8 \cdot 0.5$ C₆H₆), 1492.83 g/mol: C, 34.60; H, 6.68; N, 7.51. Found: C, 33.68; H, 6.57; N, 7.26.

Pt[Sn(NtBu)₂SiMe₂]₂Cl₂ (9**):** orange-yellow crystals; yield 2.31 g (75%); mp 320 °C dec; molecular weight (cryoscopic) 1577 g/mol.

Table 5. Selected Bond Lengths (Å) and Bond Angles (deg) of **11**

Pd(3)–Pd(4)	2.583	Sn(2)–N(4)	2.082(9)
Pd(1)–Pd(2)	2.597	P(1)–C(21)	1.830(11)
Pd(1)–P(1)	2.290(5)	P(2)–C(27)	1.841(12)
Pd(1)–Sn(1)	2.697(2)	P(3)–C(33)	1.823(10)
Pd(2)–P(2)	2.298(5)	P(4)–C(39)	1.824(11)
Pd(2)–Sn(1)	2.720(2)	Si(1)–N(1)	1.720(10)
Sn(1)–N(2)	2.050(9)	Si(1)–N(2)	1.728(10)
Sn(1)–N(1)	2.081(9)	Si(1)–C(12)	1.861(14)
Pd(3)–P(3)	2.288(5)	Si(1)–C(11)	1.870(12)
Pd(3)–Sn(2)	2.725(2)	Si(2)–N(3)	1.694(10)
Pd(4)–P(4)	2.292(5)	Si(2)–N(4)	1.738(10)
Pd(4)–Sn(2)	2.688(2)	Si(2)–C(20)	1.871(14)
Sn(2)–N(3)	2.074(9)	Si(2)–C(19)	1.874(14)
P(1)–Pd(1)–Sn(1)	118.71(4)	C(21)#1–P(1)–C(21)	102.8(4)
Sn(1)–Pd(1)–Sn(1)#1	98.85(5)	C(21)–P(1)–Pd(1)	115.5(3)
P(2)–Pd(2)–Sn(1)	118.83(4)	C(27)–P(2)–C(27)#1	101.8(5)
Sn(1)#1–Pd(2)–Sn(1)	98.70(5)	C(27)–P(2)–Pd(2)	116.4(4)
N(2)–Sn(1)–N(1)	74.5(4)	C(33)#1–P(3)–C(33)	103.1(4)
N(2)–Sn(1)–Pd(1)	146.1(3)	C(33)–P(3)–Pd(3)	115.3(3)
N(1)–Sn(1)–Pd(1)	121.0(3)	C(39)–P(4)–C(39)#1	103.2(4)
N(2)–Sn(1)–Pd(2)	126.0(3)	C(39)–P(4)–Pd(4)	115.2(4)
N(1)–Sn(1)–Pd(2)	148.5(3)	N(1)–Si(1)–N(2)	93.0(4)
Pd(1)–Sn(1)–Pd(2)	57.54(6)	N(1)–Si(1)–C(12)	115.8(6)
P(3)–Pd(3)–Sn(2)	119.20(4)	N(2)–Si(1)–C(12)	113.6(6)
Sn(2)–Pd(3)–Sn(2)#1	98.22(5)	N(1)–Si(1)–C(11)	112.8(6)
P(4)–Pd(4)–Sn(2)	117.74(4)	N(2)–Si(1)–C(11)	114.9(6)
Sn(2)#1–Pd(4)–Sn(2)	100.08(5)	C(12)–Si(1)–C(11)	106.8(6)
N(3)–Sn(2)–N(4)	74.1(4)	N(3)–Si(2)–N(4)	93.8(4)
N(3)–Sn(2)–Pd(4)	150.9(3)	N(3)–Si(2)–C(20)	113.7(6)
N(4)–Sn(2)–Pd(4)	126.5(3)	N(4)–Si(2)–C(20)	112.9(6)
N(3)–Sn(2)–Pd(3)	121.8(3)	N(3)–Si(2)–C(19)	113.2(6)
N(4)–Sn(2)–Pd(3)	142.4(3)	N(4)–Si(2)–C(19)	116.3(6)
Pd(4)–Sn(2)–Pd(3)	56.94(6)		

¹H-NMR (benzene): 0.403 (s, 1.0, Si–CH₃), 0.480 (s, 1.0, Si–CH₃), 1.415 (s, 6.0, C–CH₃) ppm. ¹³C-NMR (benzene): 6.80 (s, 1.0, Si–CH₃), 7.78 (s, 1.0, Si–CH₃), 36.65 (s, 6.0, C–CH₃), 52.78 (s, 2.0, C–CH₃) ppm. ¹¹⁹Sn-NMR (benzene): 7.17 ppm (*J*_{Pt–Sn} = 14017 Hz, 33%). ¹⁹⁵Pt-NMR (benzene): –3456.2 ppm (*J*_{Sn–Pt} = 13401 Hz, *J*_{Sn–Pt} = 14037 Hz). Anal. Calcd for C₄₀H₉₆Cl₂N₈PtSi₄Sn₄, 1542.43 g/mol: C, 31.15; H, 6.27; N, 7.56. Found: C, 31.55; H, 6.27; N, 6.89.

Reaction of Ni[Sn(NtBu)₂SiMe₂]₄ with Br₂ and PhMe₃NBr₃. A 0.67 g (0.5 mmol) sample of Ni[Sn(NtBu)₂SiMe₂]₄² was dissolved in 10 mL of hexane to which an equimolar solution of Br₂ or phenyltrimethylammonium tribromide⁷ in 20 mL of hexane was dropped at –78 °C. The reaction mixture turned dark red. After separation of some solid material, which contained NiBr₂ and SnBr₂ as found by X-ray powder diffraction, partial removal of hexane *in vacuo* yielded a concentrated solution from which crystals were obtained at –30 °C. Within these crystals two different species could easily be recognized: one species was dark red and rod-shaped, and the other one was pale yellow. The dark red crystals were identified to be Ni[Sn(NtBu)₂SiMe₂]₄·Br₂ from ¹H-NMR in benzene and from the X-ray pattern of the single crystal; yield 20 mg (2.8%). The pale yellow crystals were identified as Me₂Si(NtBu)₂SnBr₂ (0.27 g, 28%). From the remaining solution the solvent was completely removed and replaced by 1.5 mL of toluene. After crystallization at –30 °C, 0.30 g (29%) of Me₂Si(NtBu)₂Sn(NtBu)₂SiMe₂ was obtained and identified by physical and spectroscopic means.⁵

Me₂Si(NtBu)₂SnBr₂: pale yellow crystals; mp 160 °C dec. ¹H-NMR (benzene): 0.46 (s, 1.0, Si–CH₃), 1.43 (s, 3.0, C–CH₃); ¹³C-NMR: 7.847 (s, 6H, Si–CH₃), 37.083 (s, 18H, C–CH₃), δ = 54.184 (s, 2H, C–CH₃) ppm. Anal. Calcd for C₁₀H₂₄Br₂N₂SiSn, 478.92 g/mol: C, 25.08; H, 5.05; N, 5.85. Found: C, 25.37; H, 4.98; N, 5.91.

Synthesis of Rh[Ge(NtBu)₂SiMe₂]₄Cl. To a solution of 0.82 g (0.89 mmol) of Rh(PPh₃)₃Cl⁸ in 50 mL of toluene was added 0.88 mL (3.54 mmol) of Me₂Si(NtBu)₂Ge dropwise, and the solution was stirred for 2 h at room temperature and 6 h at 80 °C. After filtration the solution

was reduced to half of its volume by condensation *in vacuo*. Crystallization at –20 °C yielded 1.11 g (95%) of dark red prisms.

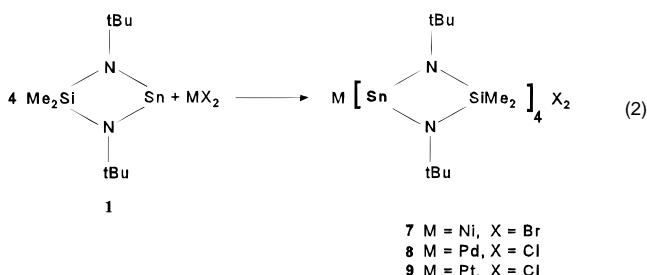
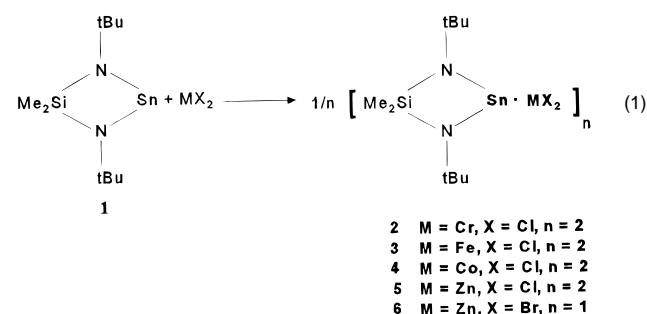
Rh[Ge(NtBu)₂SiMe₂]₄Cl·C₇H₈: mp 285 °C dec; molecular weight (cryoscopic) 1280 g/mol. MM (spectrum): highest mass 1230, calculated for C₄₀H₉₆ClGe₄N₈RhSi₄ (M – C₇H₈⁺). ¹H-NMR (benzene): 0.43 (s, 1.0, Si–CH₃), 1.50 (s, 3.0, C–CH₃) ppm. ¹³C-NMR: 5.92 (s, 2.0, Si–CH₃), 35.65 (s, 6.0, C–CH₃), 53.06 (s, 2.0, C–CH₃) ppm. ¹⁵N-NMR: –248.97 ppm. ²⁹Si-NMR: 11.75 ppm. Anal. Calcd for C₄₇H₁₀₄ClGe₄N₈RhSi₄, 1322.47 g/mol: C, 42.68; H, 7.92; N, 8.47; Cl, 2.7. Found: C, 40.60; H, 7.91; N, 7.55; Cl, 3.2.

Synthesis of Pd₂[Sn(NtBu)₂SiMe₂]₃(PPh₃)₂. In a 100 mL two necked flask equipped with a stirring bar, 0.441 mmol of Pd(PPh₃)₄ was dissolved in 20 mL of toluene to give a yellow-brown solution. Addition of 6 mL 0.44 M Sn(NtBu)₂SiMe₂ in toluene solution resulted in a rapid darkening of the reaction mixture. The solution was then stirred for 16 h at 50–60 °C. Upon removal of the solvent and excess stannylene, beautifully developed dark red crystals were formed on the walls of the flask. These crystals were redissolved in a minimum amount of toluene and the ensuing solution was cooled to 0 °C. After 3 days a large crop (0.623 g, 82%) of cherry red block-shaped crystals could be obtained.

Pd₂[Sn(NtBu)₂SiMe₂]₃(PPh₃)₂: mp 275 °C. ¹H-NMR (benzene): 0.57 (s, 18, Si–CH₃), 1.125 (s, 54, C–CH₃), 6.90–7.50 (m, 30, aromatic, partially observed) ppm. ³¹P-NMR (THF): –109.9 ppm (*J*_{117/119Sn–³¹P} = 70 Hz, 32%). Anal. Calcd for C₆₆H₁₀₂N₆P₂Pd₂Si₃Sn₃, 1694.76 g/mol: C, 46.78; H, 6.07; N, 4.96. Found: C, 46.98; H, 5.82; N, 4.85.

Results and Discussion

Syntheses. The reactions between transition metal dihalides and the cyclic bis(amino)stannylene **1** can be separated into two distinct classes. Chromium dichloride, iron dichloride, cobalt dichloride, zinc dichloride and zinc dibromide react with 1 equiv of stannylene, whereas nickel dibromide, palladium dichloride, and platinum dichloride react with 4 equiv of **1** (eq 1 and 2).



No reaction could be observed between nickel dichloride and the stannylene **1**. In all other cases the suspension of the metal dihalide in the aromatic solvent cleared up when **1** was added and the solution changed its color. Compounds **2–9** could be isolated by crystallization in high yields. By cryoscopic molecular weight determination in benzene it could be shown that the molecules **2–5** were dimeric whereas **6–9** were found to be monomeric in benzene. Compounds **2–4** are paramagnetic and no NMR spectra could be obtained for these

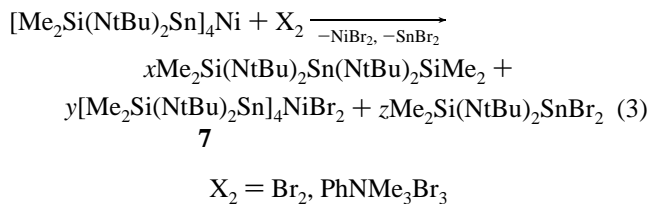
(7) Marquet, A.; Jacques, J. *Tetrahedron Lett.* **1959**, 9, 24.

(8) Young, J. F.; Osborne, J. A.; Jardine, F. H.; Wilkinson, G. J. *J. Chem. Soc., Chem. Commun.* **1965**, 131.

molecules; we used Evans' NMR-method⁹ to determine the susceptibility in solution from which the following μ_{eff} (magnetic moments) could be calculated (the values are related to the monomeric unit): **2**, 2.5 μ_{B} ; **3**, 5.5 μ_{B} ; **4**, 5.0 μ_{B} . The values for **3** and **4** compare well with those for the high spin d^6 and d^7 configuration in trigonal bipyramidal or octahedral environments (Fe^{2+} ; 5.06–5.26;^{10,11} Co^{2+} , 4.5–4.8^{12–14}), while the value for **2** seems to indicate a low spin complex (for the facile transition of high spin $\text{Cr}[d^4]$ to low spin see ref 15.). Unfortunately we could get no single crystals of compound **2** suitable for X-ray diffraction analysis. As expected the compounds **5** and **6** show no paramagnetism ($\text{Zn } d^{10}$), and the ^1H NMR spectra have two different resonance lines for the dimethylsilyl groups. This may be taken as a hint that the $\text{Me}_2\text{Si}(\text{NtBu})_2\text{Sn}$ unit is asymmetrically coordinated to the ZnCl_2 or ZnBr_2 parts of the molecule. In each case the *tert*-butyl groups show up as a common resonance. This is in contrast to the crystal structure of **5** which displays two chemically different *tert*-butyl groups (see next section). We may conclude that either the molecules show fluxional behavior in solution or the structures in solutions are different from the solid state.

From the compounds **7–9** very simple NMR spectra can be obtained, consistent with a high symmetry of these compounds in solution (the $\text{Me}_2\text{Si}(\text{NtBu})_2\text{Sn}$ part has a 2-fold symmetry and all four ligands are equivalent on the NMR time scale). As we had no problems in obtaining the NMR spectra, the paramagnetism for these d^8 systems is expected to be zero or very small. We were able to find a very small μ_{eff} value for **7** (0.2 μ_{B}) by the Evans method. This value, which is different from zero, is in accord with the crystal structure determination of **7** and **8**: in each case the transition metal is not in a perfect square planar arrangement, but deviates by a small amount (see next section). The high coupling constants $J_{\text{Sn-Pt}} \approx 14\,000$ Hz in the Sn and Pt spectra indicate direct Sn–Pt bonding.

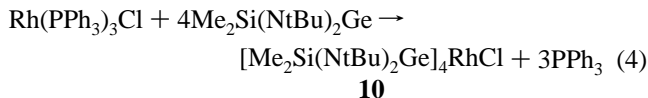
In order to test if the compound **7** may also be produced by direct interaction of the nickel(0) complex $\text{Ni}[\text{Sn}(\text{NtBu})_2\text{SiMe}_2]_4$ with the corresponding halogen or with $\text{PhMe}_3\text{NBr}_3$, we have performed the reactions in eq 3 in hexane solutions. The main



products of these reactions are the well-known spiro tetrakis(amino)stannane $\text{Me}_2\text{Si}(\text{NtBu})_2\text{Sn}(\text{NtBu})_2\text{SiMe}_2^5$ and the bis(amino)tin dibromide $\text{Me}_2\text{Si}(\text{NtBu})_2\text{SnBr}_2$, along with NiBr_2 and SnBr_2 , which precipitate from the solution and which are identified as components of the solid residue by X-ray powder diffraction. The nickel–tin cluster is thus completely degraded to its oxidation products. The spiro compound is known to be formed from $\text{Me}_2\text{Si}(\text{NtBu})_2\text{SnX}_2$ and free $\text{Sn}(\text{NtBu})_2\text{SiMe}_2$.¹⁶ Besides these main products **7** is formed in low yield and could

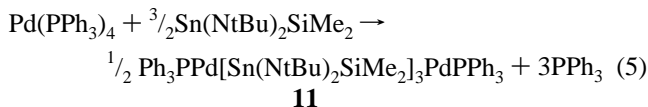
be obtained by crystallization from the solution. Carrying out the reactions in eq 3 at low temperatures does not considerably influence the ratio of the products. It is nevertheless remarkable that to a small extent the starting cluster compound can be oxidized to **7** without decomposition.

In order to establish that $\text{Me}_2\text{Si}(\text{NtBu})_2\text{Ge}$ may also coordinate efficiently to transition metals in the place of $\text{Me}_2\text{Si}(\text{NtBu})_2\text{Sn}$, we have reacted, in analogy to previous experiments,¹ Wilkinson's catalyst $\text{Rh}(\text{PPh}_3)_3\text{Cl}$ with a bis(amino)germylene (eq 4).



The reaction proceeds smoothly and the triphenylphosphine ligands at rhodium are completely displaced. To our surprise, not five carbene analogues are coordinated to rhodium as in the case of the stannylene,¹ but only four. In solution the structure of **10** seems to be highly symmetrical as may be concluded from the NMR spectra as no differences are found between the bis(amino)germylene ligands which have no interaction with chlorine and those which coordinate rhodium and chlorine at the same time (compare with the crystal structure of **10** in the next section). As a complete chloride dissociation in benzene seems to be highly improbable, we may attribute this higher symmetry of **10** in solution to fast chlorine exchanges between the molecules or to fluxional processes within **10**.

Another attempt to displace the phosphine ligands at a transition metal (this time in the oxidation state 0) by carbene like stannylenes was performed with $\text{Pd}(\text{PPh}_3)_4$ (eq 5). In the



product **11**, which is obtained in high yield, a triphenylphosphine ligand is still present. Three of the phosphine ligands are thus replaced by stannylenes, but as will become evident from the X-ray structure determination (see below) all tin atoms are involved in bridging the two palladium atoms. The NMR spectra are consistent with the solid structure of compound **11** and have a precedence with the platinum compound $\text{Ph}_3\text{P}[\text{Pt}(\text{Sn}(\text{NtBu})_2\text{SiMe}_2)_3\text{Pt}(\text{PPh}_3)]_3$, described by Stobart et al. in 1982.¹⁷

Structures of the Compounds. X-ray structure determinations on single crystals of **4**, **5**, **7**, **8**, **10**, and **11** have been performed (see Experimental Section). In Figures 1 and 2 the molecular structures of **4** and **5** are depicted, while some important molecular dimensions of these molecules are assembled in Table 2. Molecule **3** seems to be isostructural to **4** as may be deduced from the cell parameters and the crystal lattice symmetry. The common feature of these two molecules is a centrosymmetric four-membered dimetal dihalogen cycle. The bond distances and angles within these roughly square planar rings are similar, the distortion in **4** being rhomboidal and in **5** rectangular. This four membered central unit is connected through Co to a polycyclic $\text{CoN}_2\text{ClSiSn}$ unit in **4** whereas in **5** Zn is a spiro center to another four membered ZnClNSn ring which shares an edge with an SnN_2Si cycle. The $\text{SiN}_2\text{SnCoCl}$ assembly in **4** resembles a highly symmetric twistane and is isostructural to the $\text{SiN}_2\text{Sn}_2\text{Cl}$ cage found in $\text{Me}_2\text{Si}(\text{NtBu})_2\text{Sn}_2\text{Cl}^+\text{SnCl}_3^-$ (see ref 3). Comparing Figure 1 and Table 2 it is evident that the point symmetry of the molecule outside the lattice should be $2/m$ (C_{2h}) and the symmetry

(9) Evans, D. F. *J. Chem. Soc.* **1959**, 2003.

(10) Ciampolini, M.; Nardi, N. *Inorg. Chem.* **1967**, *6*, 445.

(11) Fallon, G. D.; Nichols, P. J.; West, B. O. *J. Chem. Soc., Dalton Trans.* **1986**, 2271.

(12) Kaden, T.; Hohnquist, B.; Vallee, B. L. *Inorg. Chem.* **1974**, *13*, 2585.

(13) Fox, D. B.; Hall, J. R.; Plowman, R. A. *Austr. J. Chem.* **1965**, *18*, 691.

(14) Che, C. M.; Mak S.-T.; Mak, T. C. W. *Inorg. Chem.* **1986**, *25*, 4705.

(15) Reed, C. A.; Kouba, J. K.; Grimes C. J.; Cheung, S. K. *Inorg. Chem.* **1978**, *17*, 2666.

(16) Veith, M.; Recktenwald, O.; Humpfer, E. Z. *Naturforsch.* **1978**, *B 33*, 14.

(17) Bushnell, G. W.; Eadie, D. T.; Pidcock, A.; Sam, A. R.; Holmes-Smith, R. D.; Stobart, S. R. *J. Am. Chem. Soc.* **1982**, *104*, 5837.

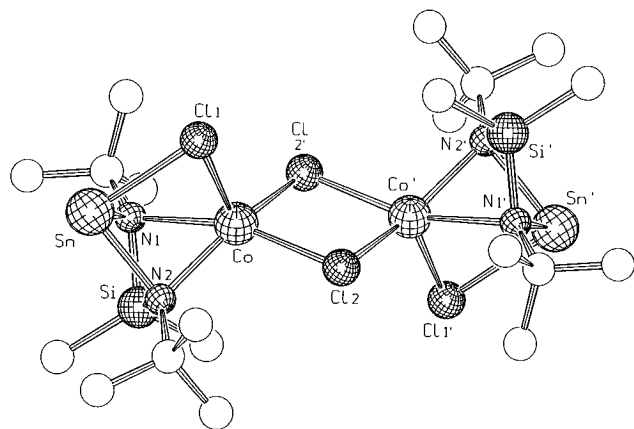


Figure 1. SCHAKAL drawing of $[\text{Me}_2\text{Si}(\text{NtBu})_2\text{Sn}]_2\text{Co}_2\text{Cl}_4$ (**4**). The nonnumbered atoms are carbon atoms; the hydrogen atoms are not drawn.

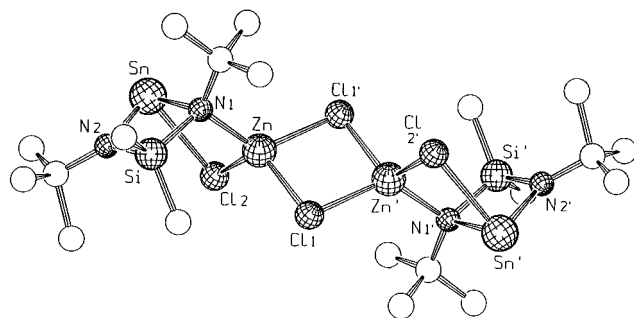


Figure 2. SCHAKAL drawing of $[\text{Me}_2\text{Si}(\text{NtBu})_2\text{Sn}]_2\text{Zn}_2\text{Cl}_4$ (**5**). The nonnumbered atoms are carbon atoms; the hydrogen atoms are omitted.

reduction in the solid should be due to the packing requirements. In the zinc compound **5** the metal atom is approximately tetrahedrally coordinated by three chlorine and one nitrogen atom. In contrast to **4** the bis(amino)stannylene unit in **5** acts only as a double Lewis acid–base system *via* the tin and one nitrogen atom toward the Zn–Cl(2) part whereas it acts as a tridentate ligand toward Co–Cl(1) in **4**. The consequence of the different ligating properties of $\text{Me}_2\text{Si}(\text{NtBu})_2\text{Sn}$ in **4** and **5** can be seen from the sum of the angles around the nitrogen atoms (for example N(2) in **5** summing up to 359.2°) or from the distances N–Sn and N–Co or N–Zn (compare Table 2). The N–Zn distances are typical for four coordinate zinc¹⁸ whereas the Co–N bond lengths are longer than expected.¹⁸ The remarkable difference in Co–N(1) and Co–N(2) bond lengths is a reflection of the different pyramidalities at N(1) and N(2) (sum of bond angles without Co at N(1) 246.7° , at N(2) 243.4°). The coordination sphere of cobalt in **4** may best be described by a distorted square pyramid, N(1), N(2), Cl(2), and Cl(2') forming the basal plane. The cobalt and zinc distances to chlorine (mean values: **4**, 2.360 Å; **5**, 2.328 Å) are within the standard values.^{18,19}

The crystal structures of **7** and **8** are isotypic, the structures of the molecules being displayed in Figures 3 and 4 and the most important distances and angles in table 3. The quality of the crystals from **8** has been superior to **7**; this difference is mostly due to librations of the *tert*-butyl groups which are more important in the nickel case. In the molecules **7** and **8**, the transition metal elements are situated almost in the center of a rectangle made up of four tin atoms the smaller edge of this Sn_4 rectangle being almost symmetrically bridged by a halogen atom. None of the nitrogen atoms are interacting with the

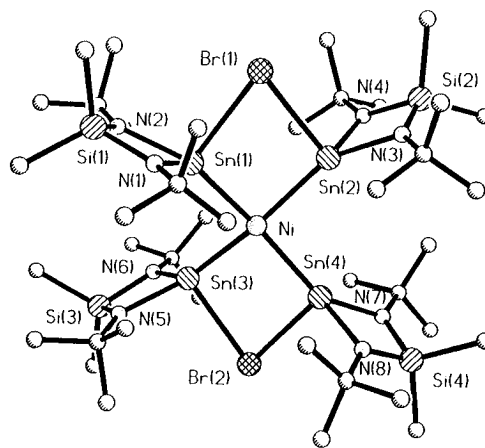


Figure 3. Drawing of $[\text{Me}_2\text{Si}(\text{NtBu})_2\text{Sn}]_4\text{NiBr}_2$ (**7**). The balls without numbering represent carbon and nitrogen atoms.

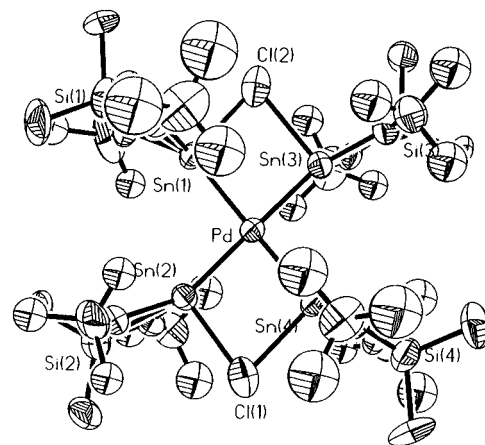


Figure 4. ORTEP drawing of $[\text{Me}_2\text{Si}(\text{NtBu})_2\text{Sn}]_4\text{PdCl}_2$ (**8**). The ellipsoids without numbering represent carbon and nitrogen atoms.

transition metals, and the SnN_2Si rings are almost perpendicularly oriented to the MSn_4X_2 plane. In each of the crystal structures a benzene molecule is situated on an inversion center of the lattice completing the crystal structure as a space filler. The molecules have no crystallographic point symmetry. This has a consequence for the crystal packing in this space group, the molecules lining up to form a helical arrangement.

The central Sn_4M metal cluster is not planar. Its deviation is seen in the Sn(1)–M–Sn(4) and Sn(3)–M–Sn(2) angles with the following values: **7**, $162.9, 163.7^\circ$; **8**, $164.5, 165.3^\circ$. The deviation from the ideal value of 180° is more important in the case of nickel compared to the palladium derivative and correlate to a smaller Ni–Sn bond [mean: 2.463(3) Å] and a longer Pd–Sn bond [mean: 2.544(2) Å]. The four tin–metal bonds are equal within standard errors in both cases and are larger compared to other tin–nickel² or similar compared to other tin–palladium bonds²⁰ of homoleptic complexes with three-coordinate tin. In comparison to $\text{Ni}[\text{Sn}(\text{NtBu})_2\text{SiMe}_2]_4$ (Ni–Sn, 2.394(2) Å; Sn–N, 2.055(9) Å)² the oxidation product **7** has longer Sn–Ni bond lengths as the coordination number at tin is raised; contrarily the Sn–N bonds in **7** seem to be comparatively short (mean in **7**: 2.02 Å). The small deviation from planarity in the clusters seem to explain in part the low paramagnetism found in solutions of **7** in which we can assume the atoms within the molecules to librate more freely.

The bromine and chlorine atoms in **7** and **8** are far away from the transition metals and are equidistant to the tin atoms to which

(18) Shannon, R. D. *Acta Crystallogr.* **1976**, A32, 751.

(19) Olmstead, M. M.; Power, P. P.; Sigel, G. *Inorg. Chem.* **1986**, 25, 1027.

(20) Hitchcock, P. B.; Lappert, M. F.; Misra, M. C. *J. Chem. Soc., Chem. Commun.* **1985**, 863.

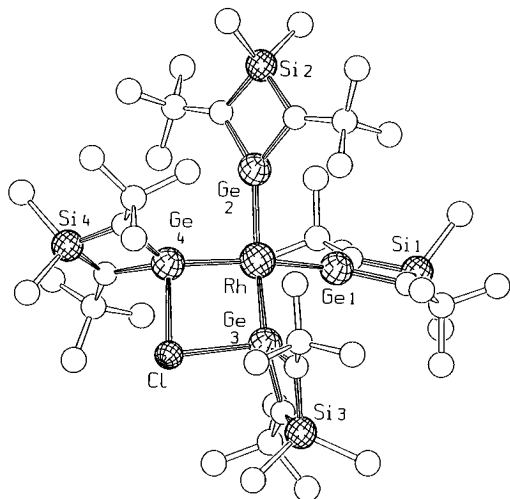


Figure 5. SCHAKAL drawing of $[\text{Me}_2\text{Si}(\text{NtBu})_2\text{Sn}]_4\text{RhCl}$ (**10**). The balls without numbering are carbon and nitrogen atoms.

they are coordinated [deviation from symmetrical bridge in **7**, 0.048 Å; in **8**, 0.0455 Å (mean values)]. The Sn–X–Sn angles are remarkably small (**7**, 75.35°; **8**, 81.47°) whereas the mean Sn–Cl (2.657(20) Å) distances are comparable to values found in Sn_2Cl_5^- anions (2.695 Å, Sn–Cl–Sn 105.5°).²¹

There is another feature of the structures of **7** and **8** which should be pointed out: the deviation from planarity of the metal cluster also has consequences on the $\text{Sn}(\text{NtBu})_2\text{-SiMe}_2$ ligands. Looking at Figure 4 it becomes clear that *tert*-butyl groups of *trans* bis(amino)stannylenes are touching one another.

On the basis of the crystal structures the cluster compounds **7–9** can be described in two ways: either M^{2+} ions are coordinated by two $\text{Me}_2\text{Si}(\text{NtBu})_2\text{Sn-X-Sn}(\text{NtBu})_2\text{SiMe}_2^-$ anions or the $[\text{Me}_2\text{Si}(\text{NtBu})_2\text{Sn}]_4\text{M}^{2+}$ cation has two further X^- anions as counterparts. Any of these descriptions are of course to be considered as borderline cases and the charge separation into anions and cations is merely formal. The structural change from $[\text{Me}_2\text{Si}(\text{NtBu})_2\text{Sn}]_4\text{Ni}$ to $\text{Br}_2[\text{Me}_2\text{Si}(\text{NtBu})_2\text{Sn}]_4\text{Ni}$ (**7**) is at the transition metal and is accompanied by a change of the coordination site: where it changes from tetrahedral to almost square planar.

In Figure 5 the molecular structure of $[\text{Me}_2\text{Si}(\text{NtBu})_2\text{Ge}]_4\text{RhCl}$ is drawn while the most important bond lengths and angles in **10** are assembled in Table 4. The molecule crystallizes with a toluene molecule serving as a space filler in the lattice. Rhodium is almost in the center of a slightly distorted planar germanium square one edge of this square being bridged by a chlorine atom. Two of the bis(amino)germylene cycles are almost perpendicular to that plane [rings with Ge(3) and Ge(4)] while the other two are severely tilted. The deviation from planarity may again be expressed by the angles Ge(1)–Rh–Ge(4) [163.36(2)°] and Ge(2)–Rh–Ge(3) [161.34(2)°]. These values compare well with the deviations found for the corresponding Sn–M–Sn angles in **7** and **8** (see above). The four germanium–rhodium bonds can be divided into two smaller ones with three coordinate germanium atoms [mean: 2.337(1) Å] and two larger ones with the tetracoordinate germanium atoms Ge(3) and Ge(4) [mean: 2.373(2) Å]. The two chlorine germanium bonds are equal within standard errors [mean: 2.599(3) Å] and the Ge–Cl–Ge angle [77.34(4)°] is acute like the corresponding Sn–X–Sn angles in **7** or **8**. As expected, the Ge–N bonds adjacent to the chlorine bridge [mean: 1.851

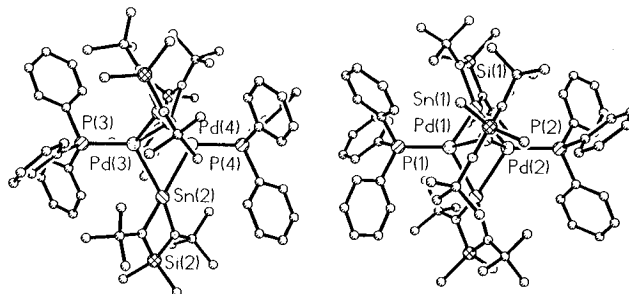


Figure 6. Drawing of the two enantiomeric molecules of $\text{Ph}_3\text{PPd}[\text{Sn}(\text{NtBu})_2\text{SiMe}_2]_3\text{PdPPh}_3$ in the crystal structure of **11**. Only heavy atoms have been numbered in part. A 3-fold crystallographic axis runs through P(3)–Pd(3)–Pd(4)–P(4) and P(1)–Pd(1)–Pd(2)–P(2), respectively.

(2) Å] are considerably longer than those which have no chlorine atom coordinated to germanium [mean: 1.836(2) Å].

From a structural point of view the structures of **7**, **8** (presumably also **9**, see Experimental Section), and **10** compare well, as the inner metal cores MM'_4 (M = transition metal, M' = Ge or Sn), which approaches a cross-bar, are apparently similar. The deviations from planarity are also analogous to one another and may be attributed to the steric bulkiness of the $\text{Me}_2\text{Si}(\text{NtBu})_2\text{El}$ ligands. In all compounds no interaction of the nitrogen atoms of the rings is observed with the transition metal elements. It is interesting to note that the analogous compound with Rh(I) and $\text{Sn}(\text{NtBu})_2\text{SiMe}_2$ ligands to **10** has a different composition $\{[\text{Me}_2\text{Si}(\text{NtBu})_2\text{Sn}]_5\text{RhCl}\}$ and structure: rhodium is in the center of a trigonal bipyramid of tin atoms.¹ We ascribe this to the less space demanding property of $\text{Me}_2\text{Si}(\text{NtBu})_2\text{Sn}$, the Sn–N bond [mean 2.06 Å] being approximately 0.2 Å longer than in $\text{Ge}(\text{NtBu})_2\text{SiMe}_2$ and the Rh–Sn distance [mean 2.55 Å]¹ exceeding the Rh–Ge distances by approximately 0.20 Å. All geometries found at Ni, Pd, and Rh are consistent with a d^8 -configuration of the metallic atom.

A view of the two independent molecules present in the crystal of $\text{Ph}_3\text{PPd}[\text{Sn}(\text{NtBu})_2\text{SiMe}_2]_3\text{PdPPh}_3$, **11**, is shown in Figure 6 while some of the distances and angles within these molecules are depicted in Table 5. The two molecules are similar with respect to the inner Pd_2Sn_3 trigonal bipyramidal core coordinated at the Pd apices by Ph_3P ligands. They are different in the orientation of the four-membered $\text{Sn}_2\text{N}_2\text{Si}$ cycles with respect to Sn_3 plane: while these rings form a right-handed “paddle wheel” in the molecule with Pd(1) and Pd(2), they form a left-handed “paddle wheel” in the other molecule as may be easily deduced from inspection of Figure 6 (the dihedral angles between the two planes can be calculated to 20.7°). Also the phenyl groups on the phosphorus atoms follow in part these geometries: thus the phenyl groups on P(2) and P(3) are turned in form of a right handed “paddle wheel” while they are left handed at the P(1) and P(4) atoms. The two molecules have crystallographic C_3 symmetry and can be considered as enantiomeric forms.

In the metallic five-membered central cluster the six Sn–Pd bonds are almost equal in the molecule with Pd(1) and Pd(2) [Pd–Sn 2.697, 2.700 Å] while they are quite different in the molecule with Pd(3) and Pd(4) [Pd–Sn 2.725, 2.688 Å]. So far we have no straight forward explanation for this effect. The Sn–Pd–Sn angles in the two molecules (98.78°, 99.15°) approach 100° while the Pd–Sn–Pd angles are extremely acute (57.54°, 56.94°). This may be taken as a hint that the two palladium atoms form a Pd–Pd bonding interaction and the distances between these atoms are short [Pd(1)–Pd(2) 2.597 Å, Pd(3)–Pd(4) 2.583 Å]. Our findings resemble those obtained for $\text{Ph}_3\text{PPt}[\text{Sn}(\text{acac})_2]_3\text{PtPPh}_3$ [Pt–Pt 2.593(1) Å, Pt–Sn–Pt 57.87(3)°] and we also would like to adopt the bonding

(21) Veith, M.; Gödicke, B.; Huch, V. Z. *Anorg. Allg. Chem.* **1989**, 579, 99.

description proposed in this paper for the Pt_2Sn_3 cluster.¹⁷ Thus the Pd should retain its closed-shell d^{10} character with three hybrid orbitals on each Pd and with a single orbital at tin to give three bonding, three nonbonding, and three antibonding levels. The bonding model thus is based on a delocalization of electron density between the five metal centers.

Compared to **8** the Pd–Sn bonds in **11** are elongated by almost 0.159 Å. This is in line with the qualitative bonding description given so far: the tin atom can supply the cluster with only two electrons per atom and as two Pd centers have to be satisfied the bonding in **11** should be less efficient as compared to **8**. The electron withdrawal from tin in **11** is also observed in the Sn–N bonds in both compounds **8** (mean Sn–N 2.030(5) Å) and **11** (mean Sn–N 2.072(5) Å).

Conclusions

It has been shown that transition metal chlorides (bromide for Ni) behave differently toward $\text{Me}_2\text{Si}(\text{NtBu})_2\text{Sn}$, forming either Lewis acid–base adducts or metal clusters. $\text{Br}_2[\text{Me}_2\text{Si}(\text{NtBu})_2\text{Sn}]_4\text{Ni}$ can also be generated in low yield by treating $[\text{Me}_2\text{Si}(\text{NtBu})_2\text{Sn}]_4\text{Ni}$ with Br_2 or R_4NBr_3 , the main reaction leading to oxidative degradation of the starting compound. This

formation (although low in yield) is nevertheless remarkable as the oxidation of $[\text{Me}_2\text{Si}(\text{NtBu})_2\text{Sn}]_4\text{Ni}$ proceeds at the outer sphere of the cluster without direct Br₂–Ni interaction. At the same time the nickel atom is transferred from a tetrahedral coordination to almost square planar. Within the metal clusters having five metallic elements and $\text{Me}_2\text{Si}(\text{NtBu})_2\text{Sn}$ as components, $[\text{Me}_2\text{Si}(\text{NtBu})_2\text{Ge}]_4\text{ClRh}$ fits in nicely among $[\text{Me}_2\text{Si}(\text{NtBu})_2\text{Sn}]_4\text{Ni}$ and $[\text{Me}_2\text{Si}(\text{NtBu})_2\text{Sn}]_4\text{MX}_2$ (M = Ni, Pd, Pt). The five membered metal cluster in $\text{Ph}_3\text{PPd}[\text{Sn}(\text{NtBu})_2\text{SiMe}_2]_3\text{-PdPh}_3$ (**11**) is structurally very different from **7–10**; this can be attributed to the fact that the metal cluster is electron deficient compared to the other compounds.

Acknowledgment. We would like to thank the Fonds der Chemischen Industrie and the Deutsche Forschungsgemeinschaft (DFG) for financial support.

Supporting Information Available: Tables of X-ray experimental details, bond lengths and angles, positional parameters, and anisotropic thermal parameters for **4**, **5**, **7**, **8**, **10**, and **11** (41 pages). Ordering information is given on any current masthead page.

IC960007A